ELSEVIER

Journal of Alloys and Compounds 230 (1995) 46–52

Journal of ALLOYS AND COMPOUNDS

Formation of RE_xNi_y (RE = La, Ce, Pr or Nd) compounds by calciothermic reduction of La_2O_3, CeO_2, Pr_6O_{11} and Nd_2O_3

M. Ohtsuka[a,*], D.-Y. Kim[b], K. Itagaki[a]

[a]*Institute for Advanced Materials Processing, Tohoku University, Katahira 2-1-1, Aoba-ku, Sendai 980-77, Japan*
[b]*Metals Research and Development Center, Kia Steel Co., Ltd., Soryong-Dong 1-6, Kunsan Cheollabukdo, South Korea*

Received 1 March 1995; in final form 2 May 1995

Abstract

$LaNi_5$, $CeNi_5$, $PrNi_5$ and $NdNi_5$ powders were prepared from the corresponding oxides by a reduction–diffusion method using calcium as reductant and the morphology of the product and the mechanism of the reaction were examined. It was clarified that Ca_xNi_y compounds formed during the reaction had a significant role in the formation of RE_xNi_y. Instead of a common direct reaction of $xRE + yNi = RE_xNi_y$, an indirect substitution reaction of $aCa_xNi_y + bRE = cRE_xNi_y + dCa$ prevailed. This enhanced the rate of formation of $RENi_5$ significantly.

Keywords: Rare earth-nickel compounds; Calciothermic reduction; Reduction–diffusion method; Reaction mechanism

1. Introduction

Nickel misch metal compounds $RmNi_5$ have a favorable hydrogen absorbability and are used as hydrogen storage materials for rechargeable batteries. When considering the development of a low energy-consuming and low cost process for producing $RmNi_5$, a direct production process where misch metal oxides or halides can be converted directly to their compound powders is desirable. The typical method is a calciothermic reduction process (a reduction–diffusion (R–D) method) using metallic calcium or calcium hydride as reductant. This has been applied successfully to the production of $SmCo_5$ magnets in industry. Likewise, the present authors have conducted similar experimental studies on the calciothermic reduction of misch metal oxides and the formation of the $RmNi_5$ powders [1–3]. Notable differences in the morphology of the reacted particles and the rate of the formation of $RmNi_5$ were observed when the La-base and Ce-base oxides were used as the misch metal resources in the R–D experiments. To clarify these differences, the R–D experiments have been conducted for La_2O_3, CeO_2, Pr_6O_{11} and Nd_2O_3 which are the predominant constituents of misch metal oxide resources.

2. Experimental procedure

Rare earth (RE) oxide powders of La_2O_3, CeO_2, Pr_6O_{11} and Nd_2O_3 used in the R–D experiments were from CERAC Company (USA), having 99.9 mass% purity and were less than 45 μm in diameter. Nickel metal having 99.9 mass% purity was nearly spherical and its diameter was about 130 μm. Small chips of metallic calcium having 99.9 mass% purity with a diameter of about 2 mm were used as reductant. These components were mixed thoroughly and were pressed with a pressure of 39 MPa to make a pellet with a diameter of 12 mm and a thickness of about 5 mm. The mole ratio of RE to Ni in the pellet was adjusted to be 1 to 5 and its calcium content was kept at twice the stoichiometric required to convert the RE oxide completely to the metallic state. Two or three samples pellets were put in an MgO crucible with an inner diameter of 19 mm. The crucible was set in a quartz reaction tube filled with argon gas and put into a heated furnace. It took about 700 s for the samples to reach the pre-set temperature. The sample after react-

* Corresponding author.

SSDI 0925-8388(95)01885-9

ing for a given time was taken out of the furnace and prepared for analysis. The reacted samples mounted on resin were polished in emery paper and Al_2O_3 powder without water. The microstructure was observed by optical and scanning electron microscopy (SEM). An electron probe microanalysis (EPMA) was undertaken to determine the composition. The charge compositions and conditions for the R–D experiments are listed in Table 1.

3. Formation of La_xNi_y compounds

3.1. Morphology of reacted particles

SEM and characteristic X-ray images of Ni, La and Ca for a cross-section of the sample obtained in the R–D experiment at 1273 K for 4.3 ks are shown in Fig. 1. It is known from the images and the EPMA that multilayers of $CaNi_5$, $LaNi_5$ and La_2Ni_7 compounds are formed in this order around the unreacted nickel core. La is not found in this core and on the $CaNi_5$ layer while Ca with its dense characteristic X-ray patterns (Fig. 1(d)) is observed in the $CaNi_5$ layer. The bulk phase which exists outside the reacted particle is also mainly composed of CaO and Ca. Marginal shapes of the unreacted core and the compound layers are similar to each other. This suggests that these compounds were formed topochemically around the nickel particle during the reactive diffusion.

As listed in Table 2, La_xNi_y and Ca_xNi_y compounds, which were formed in various conditions of the R–D experiments, are different for different temperatures

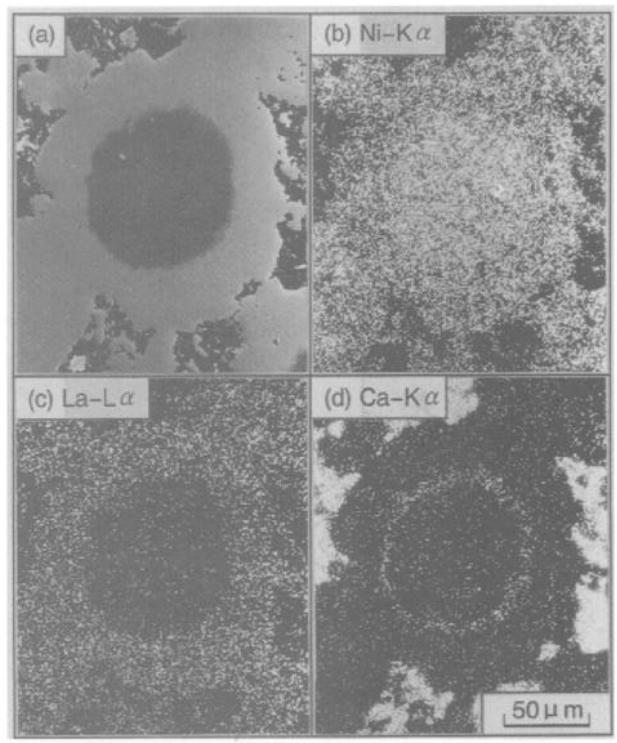

Fig. 1. (a) SEM image and (b)–(d) characteristic X-ray images in a cross-section of the sample obtained in the R–D experiment of the La–Ni system at 1273 K for 4.3 ks.

as well as for different reaction times. The La_xNi_y compounds with various mole ratios x/y were formed topochemically from inside to outside the reacted particle in the order of increasing x/y. The x/y ratios of the La_xNi_y compounds are in good agreement with a phase diagram of the La–Ni binary system reported by the present authors [4]. $CaNi_5$ is a major compound of Ca_xNi_y. It was always sandwiched between the unreacted nickel core and the $LaNi_5$ layer during the reactive diffusion and shifted toward the inner part as the reaction proceeded. Once the nickel core was dissolved, the central part of the reacted particle was occupied by $CaNi_5$ and other Ca_xNi_y compounds such as $CaNi_2$ and $CaNi_3$. In the final reaction stage, these Ca_xNi_y compounds were converted to $LaNi_5$ by the La atoms diffusing into the central part of the particle. It is considered that the liberated Ca metal flowed out of the particle through its cracks because only a vacant hole remained in the central part at the end of the R–D reaction. Fig. 2 shows a microphotograph of the sample obtained at 1273 K for 7.9 ks where the reaction time is long enough for the R–D reaction to reach completion. The reacted particles with a small hole in its central part correspond to $LaNi_5$. These particles are dotted in the bulk phase which is composed of Ca and CaO.

Table 1
The charge compositions and conditions for the R–D experiments

System	Charge compositions	Temperature T (K)	Holding time t (ks)
La–Ni		1123	
	5.9 mol.% La_2O_3	1173	
	58.8 mol.% Ni	1223	0.7 1.3 2.5 4.3
	35.3 mol.% Ca	1273	
		1323	
Ce–Ni	10.0 mol.% Ce_2O_2	1123	0.7 2.5
	50.0 mol.% Ni	1223	2.5
	40.0 mol.% Ca	1273	1.9 4.3
Pr–Ni	1.9 mol.% Pr_6O_{11}	1123	0.7 2.5
	56.6 mol.% Ni	1223	2.5
	41.5 mol.% Ca	1273	1.9 4.3
Nd–Ni	5.9 mol.% Nd_2O_3	1123	0.7 2.5
	58.8 mol.% Ni	1223	2.5
	35.3 mol.% f Ca	1273	1.9 4.3

Table 2
RE_xNi_y and Ca_xNi_y compounds formed in various conditions of R–D experiments

System	Temperature T (K)	RE_xNi_y	Ca_xNi_y
La–Ni	1123	$LaNi_2$ La_2Ni_5 $LaNi_3$ La_2Ni_7 $LaNi_5$	$CaNi_5$
	1173	$LaNi_3$ La_2Ni_7 $LaNi_5$	$CaNi_5$
	1223	La_2Ni_7 $LaNi_5$	$CaNi_5$
	1273	La_2Ni_7 $LaNi_5$	$CaNi_5$
	1323	La_2Ni_7 $LaNi_5$	$CaNi_2$ $CaNi_3$ $CaNi_5$
Ce–Ni	1123	$CeNi_3$ $CeNi_5$	
	1223	$CeNi_4$ $CeNi_5$	$CaNi_2$ $CaNi_3$ $CaNi_5$
	1273	$CeNi_5$	
Pr–Ni	1123	$PrNi_3$ $PrNi_5$	
	1223	$PrNi_3$ $PrNi_5$	$CaNi_2$ $CaNi_3$ $CaNi_5$
	1273	$PrNi_5$	
Nd–Ni	1123	$NdNi_2$ $NdNi_3$ Nd_2Ni_7 $NdNi_5$	
	1223	Nd_2Ni_7 $NdNi_5$	$CaNi_2$ $CaNi_3$ $CaNi_5$
	1273	Nd_2Ni_7 $NdNi_5$	

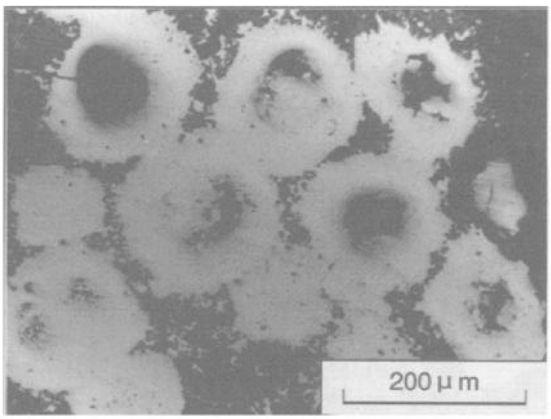

Fig. 2. Optical microphotograph in a cross-section of the sample obtained in the R–D experiment of the La–Ni system at 1273 K for 7.9 ks.

3.2. Reaction mechanism

From the observed morphology of the sample after reactive diffusion, a mechanism for the formation of La_xNi_y compounds is considered as follows.

In the initial reaction stage where the sample is being heated to the pre-set temperature, La_2O_3 is not substantially reduced by the Ca reductant. Ca reacts with the nickel particle and a $CaNi_5$ layer is produced on its surface. It was found experimentally that the formation of $CaNi_5$ proceeded remarkably in the temperature region just above the melting point of Ca (1115 K) although it started at a lower temperature around the eutectic point (878 K) of the Ca–Ni alloy.

A marked reduction in La_2O_3 can occur at a higher temperature above 1173 K and it is considered that the La produced goes into solution with the liquid Ca in the bulk phase surrounding the particle because of the wide miscibility found in the phase diagram of the La–Ca binary system [5]. Hence, the liquid calcium is considered to be a medium to transport La atoms to the nickel particle. The dissolved La reacts with the $CaNi_5$ on the nickel particle and forms La_xNi_y on the surface of the $CaNi_5$ layer, according to

$$a\mathrm{La(l, in\ La{-}Ca)} + b\mathrm{CaNi_5(s)} = c\mathrm{La_xNi_y(s,l)} + d\mathrm{Ca(l)} \quad (1)$$

Here s and l represent solid and liquid respectively. The Gibbs free-energy change of this reaction [6,7] when $La_xNi_y(s)$ corresponds to $LaNi_5(s)$ is given as $\Delta G^0\ (\mathrm{J\ mol^{-1}}) = -92760 + 12.6T\ (\mathrm{K})$. This value is highly negative at $T = 1323$ K, indicating that $LaNi_5$ is thermodynamically much more stable than $CaNi_5$.

Once an La_xNi_y layer is formed on the surface of the reacted particle, the liquid calcium in the bulk phase is difficult to diffuse into the particle because La_xNi_y has a small solubility for Ca and acts as a barrier against the diffusing Ca atoms. It is considered further that the Ca liberated in Eq. (1) diffuses through the $CaNi_5$ layer and reacts with the metallic nickel to form $CaNi_5$ at the interface between the $CaNi_5$ and nickel phases, as shown by

$$\mathrm{Ca} + 5\mathrm{Ni} = \mathrm{CaNi_5} \quad (2)$$

The substitution reaction of Eq. (1) and the $CaNi_5$-forming reaction of Eq. (2) may proceed progressively

in the process of reactive diffusion. This may result in the anomalous morphology of the reacted particle where the $CaNi_5$ layer is always sandwiched between the unreacted nickel core and the $LaNi_5$ layer. Furthermore the $CaNi_5$ shifts toward the center of the particle as the reactive diffusion proceeds.

This estimated mechanism of the indirect substitution reaction between La and Ni is quite different from the mechanism in the case without $CaNi_5$, where La and Ni react directly and make an $LaNi_5$ layer on the surface of the nickel phase according to the reaction $La + 5Ni = LaNi_5$.

3.3. Rate of formation of compounds

15 reacted particles with a diameter of about 150 μm were selected in the optical microphotograph of a sample pellet after the R–D experiment. The averaged volume fractions $\alpha(i)$, of the unreacted nickel core, the $CaNi_5$ layer and the La_xNi_y layers were determined using an image processor analyzer based on a spherical approximation:

$$\alpha(i) = \frac{V(i)}{V(\mathrm{Ni}) + V(\mathrm{CaNi_5}) + V(\mathrm{La_xNi_y})} \quad (3)$$

Here $V(\mathrm{Ni})$ and $V(\mathrm{CaNi_5})$ are the volumes of the nickel core and the $CaNi_5$ layer and $V(La_xNi_y)$ is the sum of the volumes of the La_xNi_y layers.

$\alpha(i)$ curves plotted reaction time at 1273 K are shown in Fig. 3. The formation of La_xNi_y compounds is very fast and $\alpha(La_xNi_y)$ amounts to more than 0.8 in a short reaction time of 4 ks while $\alpha(CaNi_5)$ does not change much with reaction time. It was found that $\alpha(La_xNi_y)$ increased with increasing temperature.

When the interdiffusion in the $LaNi_5$ layer is considered to be the rate-controlling step in the R–D process, a relationship between the diffusion time t and the reacted fraction $\alpha(LaNi_5)$ of a spherical nickel particle where $\alpha(LaNi_5) = 1 - (r_t/r_0)^3$, is given by

$$\frac{2M\tilde{D}(C_{21} - C_{23})}{\beta\rho r_0^2} t = 1 - \tfrac{2}{3}\alpha(\mathrm{LaNi_5}) - [1 - \alpha(\mathrm{LaNi_5})]^{2/3} \quad (4)$$

provided that $LaNi_5$ is formed topochemically. In Eq. (4), M and ρ are the atomic weight and density respectively of nickel, β is a chemical coefficient for the formation of $LaNi_5$ ($\beta = \frac{1}{5}$), and r_0 and r_t are the radii of the nickel particle at the times zero and t respectively. $\tilde{D}$ is the interdiffusion coefficient in the $LaNi_5$ compound, and C_{21} and C_{23} are solubility limits of a $LaNi_5$ solid solution on the liquidus side and the nickel side respectively. $\tilde{D}$, C_{21} and C_{23} were determined experimentally at high temperatures above 1273 K by the present authors [4]. This model is similar to the unreacted core model which is used for the analysis of the rate phenomena to reduce the pellets of iron oxide with CO gas.

By substituting these values in Eq. (4), a relationship between $\alpha(LaNi_5)$ and t was calculated at 1273 K for a nickel particle with a diameter of 130 μm (r_0 = 65 μm). This is shown as a broken curve in Fig. 4 together with the experimental values obtained in the R–D experiments using the nickel particles with similar diameters. It should be noted that the calculated values are significantly lower than the experimental values. This notable discrepancy cannot be ascribed to the inadequate assumptions that were made when Eq. (4) was derived and other intrinsic reasons must be considered to explain it.

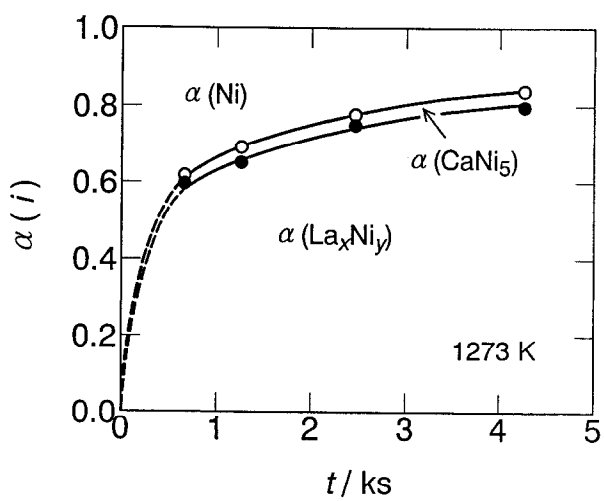

Fig. 3. Volume fractions of the unreacted nickel core, the $CaNi_5$ layer and the La_xNi_y layers of reacted particles with a diameter of about 150 μm which were obtained in the R–D experiment of the La–Ni system at 1273 K.

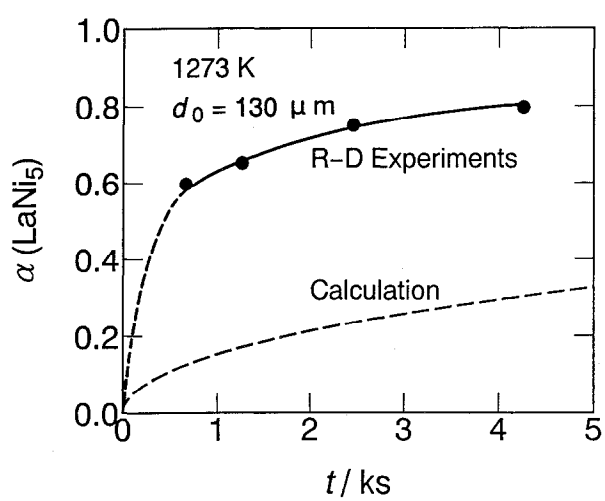

Fig. 4. Relationship between the volume fraction of the $LaNi_5$ layer of reacted particles and reaction time at 1273 K for a nickel particle with a diameter of 130 μm.

As described previously, the $CaNi_5$ compound formed in the R–D experiments was always located between the $LaNi_5$ layer and the inner unreacted nickel core. This compound is considered to play an important role in enhancing the formation of $LaNi_5$. To clarify the enhancement mechanism, the present authors [4] carried out a series of diffusion experiments for the La–Ni system at 1373 K using two kinds of diffusion couple, the Ni–(La–Ni) melt and the Ni–$CaNi_5$–(La–Ni) melt. In the latter couple, a thin $CaNi_5$ layer with a thickness of about 100 μm was coated on the surface of a nickel rod with a diameter of 5 mm by depositing calcium vapor and reacting with the nickel substrate. It was found that, in the case of the diffusion couple with the $CaNi_5$ layer, the whole nickel rod was converted into the $LaNi_5$ compound in a considerably short period of about 22 ks. This is 1/1060 of the time required for the diffusion couple without the $CaNi_5$ layer.

It can be estimated that a notable difference in crystallographic properties must exist between the $LaNi_5$ layers as a result of the direct reaction of $La + 5Ni = LaNi_5$ and the indirect substitution reaction in which $CaNi_5$ operates. A plausible explanation is that slow bulk diffusion prevails for the $LaNi_5$ layer which is produced by the direct reaction while rapid grain boundary or pore diffusion prevails for the $LaNi_5$ layer produced by the indirect reaction. Nevertheless, the reason why $CaNi_5$ enhanced the formation of $LaNi_5$ is not yet conclusive and further study will be required to clarify the diffusion mechanism more satisfactorily.

4. Formation of Ce_xNi_y, Pr_xNi_y and Nd_xNi_y compounds

4.1. Ce_xNi_y compounds

SEM and characteristic X-ray images of a cross-section of a reacted particle in the sample obtained by reducing CeO_2 at 1123 K for 2.5 ks are shown in Fig. 5, and the Ce_xNi_y and Ca_xNi_y compounds which appeared during the R–D reaction are listed in Table 2. As shown in Fig. 5(a), the two Ce_xNi_y compounds $CeNi_3$ and $CeNi_5$ with a fine grain-like structure (not a layer-like structure as in the case of reduction of La_2O_3) are formed in the outer part of the reacted particle or outside it. Some Ca_xNi_y compounds of $CaNi_2$, $CaNi_3$ and $CaNi_5$ composition with complicated shapes are scattered in the whole particle as shown in Fig. 5(d). This morphology is quite different from that observed in the reduction of La_2O_3 as shown in Fig. 4(a).

With increasing reaction time, the proportion of these Ca_xNi_y compounds decreased while that of

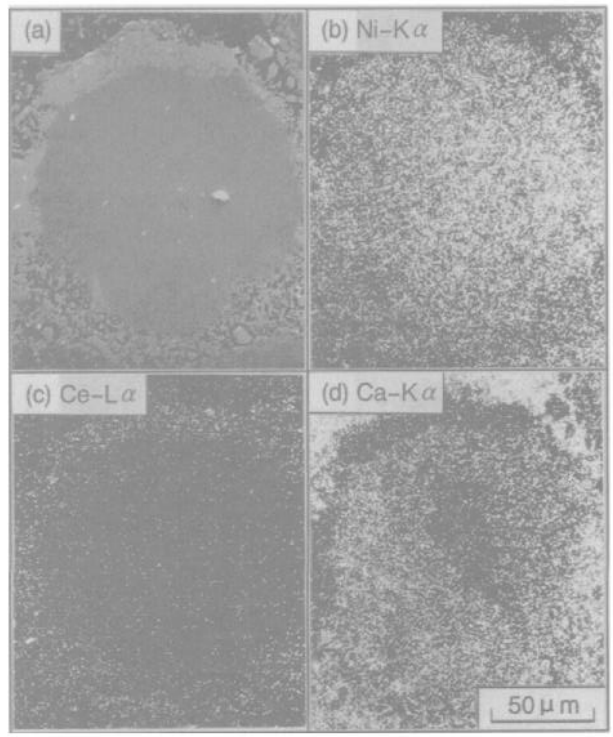

Fig. 5. (a) SEM image and (b)–(d) characteristic X-ray images in a cross-section of the sample obtained in the R–D experiment of the Ce–Ni system at 1123 K for 2.5 ks.

$CeNi_5$ increased. Fig. 6 shows a microphotograph of the sample obtained at 1273 K for 7.9 ks where the reaction time is long enough for the R–D reaction to reach completion. It is composed of a bulk phase (the black part), reacted particles and a reticulate product connecting the particles. The compositions of the particles and the reticulate product correspond to those of $CeNi_5$, indicating that all the CeO_2 and nickel reactants used in the R–D experiment were converted to $CeNi_5$ in this reaction time. Marginal shapes of the reacted particles are irregular and not semispherical as

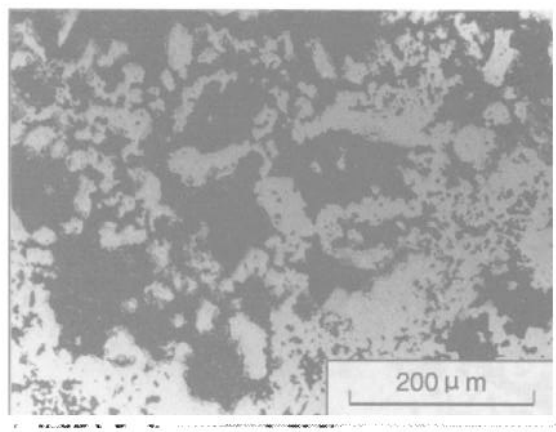

Fig. 6. Optical microphotograph in a cross-section of the sample obtained in the R–D experiment of the Ce–Ni system at 1273 K for 7.9 ks.

in the case of the reduction of La_2O_3. Each particle has a hole in its central part, which is considerably larger than that in the reduction of La_2O_3 shown in Fig. 2. It was impossible to determine the volume fractions of the compound layers by means of the image processor.

The morphology of the sample obtained in the reduction of CeO_2 indicates that the reaction mechanism is different from that in the reduction of La_2O_3. The Ce–Ca binary system [5] has a miscibility which is much smaller than that in the La–Ca system [5] and exhibits a two-liquid region in the R–D experiments at about 1223 K. This is composed of a cerium-rich phase of L_1 with about 4 mol.% Ca and a calcium-rich phase of L_2 with about 5 mol.% Ca. The reaction mechanism in the reduction of CeO_2 in coexistence with the two liquids ($L_1 + L_2$) in the bulk phase surrounding the nickel particles is considered as follows.

In the initial reaction stage where the samples is being heated to the pre-set temperature in the R–D experiment, Ca reacts with the nickel particle and a $CaNi_5$ layer is formed on its surface as in the case of the reduction of La_2O_3. With increasing temperature, the reduction of CeO_2 proceeds significantly and the two liquids L_1 and L_2 are produced in the bulk phase. At this stage, the formation of Ce_xNi_y is not remarkable because the L_2 phase with the small amount of Ce covers a portion of the surface of the particle. Furthermore, the contact of the L_1 phase having the high content of Ce to the particle is prevented by the L_2 phase surrounding the particle. Under this circumstance, the nickel particle reacts further with Ca in the bulk (L_2 phase) and forms a series of Ca_xNi_y compounds as shown in Table 2 and Fig. 5. Even dissolution of nickel in the liquid Ca(L_2 phase) is suggested by the appearance of the reticulate product outside the particles as shown in Fig. 6. The bulk phase is formed according to

$$a\mathrm{Ni(in\ Ca)} + b\mathrm{Ce(in\ Ca)} = c\mathrm{Ce}_x\mathrm{Ni}_y \quad (5)$$

It is considered that the following substitution reaction to form the Ce_xNi_y compounds occurs after most of the nickel in the particle is converted to the Ca_xNi_y compounds:

$$a\mathrm{Ca}_x\mathrm{Ni}_y + b\mathrm{Ce} = c\mathrm{Ce}_x\mathrm{Ni}_y + d\mathrm{Ca} \quad (6)$$

The possibility of this substitution reaction is also suggested by the large negative Gibbs free-energy change [6,7] for the reaction of $Ce(l) + CaNi_5(s) = CeNi_5(s) + Ca(l)$ with ΔG^0 (J mol^{-1}) $= -92050 - 8.4T$(K). The Ca liberated in Eq. (6) diffuses out of the particle and a large hole remains in its central part as shown in Fig. 6.

4.2. Pr_xNi_y compounds

SEM and characteristic X-ray images of a cross-section of the reacted particle in the reduction of Pr_6O_{11} are shown in Fig. 7, and the Pr_xNi_y and Ca_xNi_y compounds that appeared during the R–D reaction are listed in Table 2. A series of Ca_xNi_y compounds in addition to $CaNi_5$ are formed within the reacted particle, and its morphology is similar to that in the reduction of CeO_2 but is significantly different from that in the reduction of La_2O_3. This indicates that the Pr–Ca system will represent a two-liquid ($L_1 + L_2$) region at a temperature in the R–D experiments although a phase diagram of the Pr–Ca system is not reported anywhere, and that the contact of the L_1 phase having a high content of Pr to the particle is prevented by the L_2 phase which has a low content of Pr, thus allowing a fast reaction of Ca with the nickel particle prior to the formation of Pr_xNi_y compounds.

4.3. Nd_xNi_y compounds

SEM and characteristic X-ray images of a cross-section of the reacted particle in the reduction of Nd_2O_3 shown in Fig. 8 present a morphology which is very similar to that in the reductions of CeO_2 and Pr_6O_{11}. This indicates that the L_2 phase having the low content of Nd also prevents the contact of the L_1

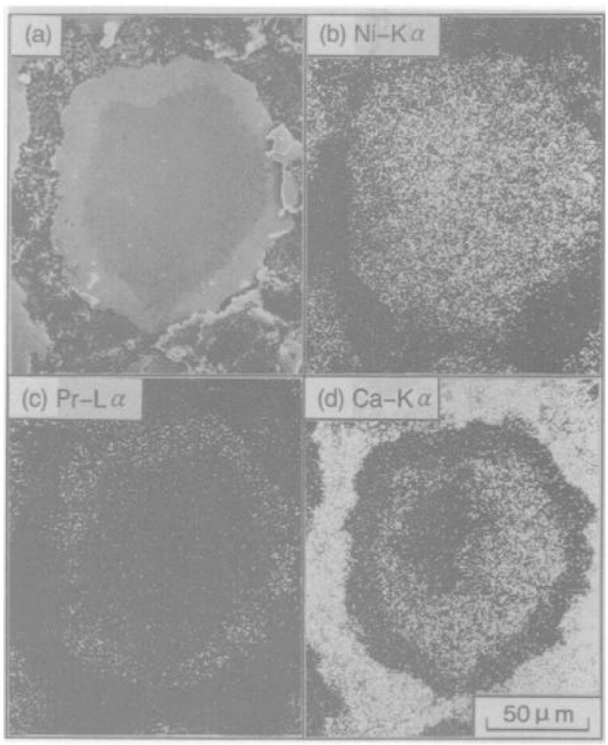

Fig. 7. (a) SEM image and (b)–(d) characteristic X-ray images in a cross-section of the sample obtained in the R–D experiment of the Pr–Ni system at 1123 K for 2.5 ks.

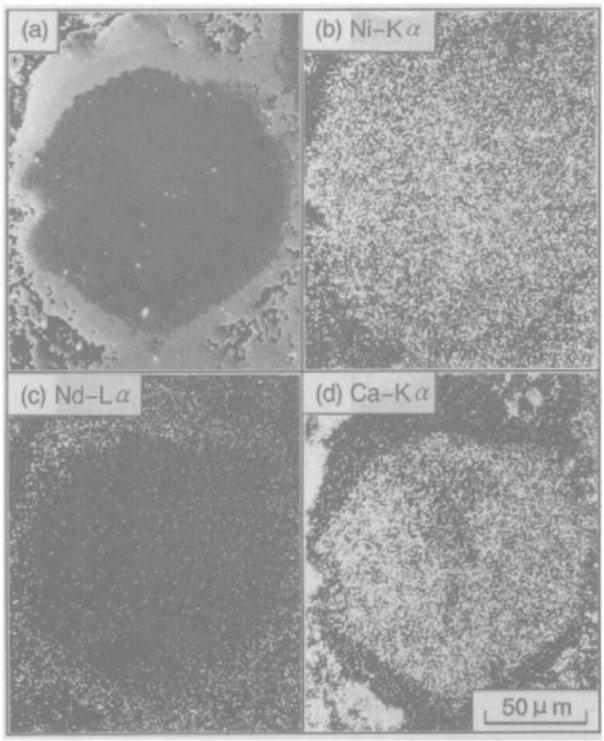

Fig. 8. (a) SEM image and (b)–(d) characteristic X-ray images in a cross-section of the sample obtained in the R–D experiment of the Nd–Ni system at 1123 K for 2.5 ks.

phase with the high content of Nd to the nickel particle as suggested by a phase diagram of the Nd–Ca binary system [5] which represents a two-liquid ($L_1 + L_2$) region at high temperatures.

5. Conclusion

The present study has clarified that Ca_xNi_y compounds formed during the R–D reaction had a significant effect on the morphology of the remaining reacted nickel particle as well as to the reaction mechanism to make $RENi_5$(RE = La, Ce, Pr or Nd). It was suggested that $RENi_5$ compounds were formed not by a common direct reaction $RE + 5Ni = RENi_5$, between RE and Ni atoms, but by a kind of indirect substitution reaction $CaNi_5 + RE = RENi_5 + Ca$, which enhanced the reaction rate significantly. It is predicted that the reaction rate in the R–D process for making $RENi_5$ powders is faster than those for making Sm–Co and Fe–Nd–B compound powders because Co and Fe are almost immiscible with Ca and do not make any compound with it. The morphology of the reacted particle can be explained primarily by a tendency to make a two-liquid region in the bulk phase composed of Ca and RE. A topochemical reaction prevailing in the reduction of La_2O_3 because the La–Ca system has a wide miscibility and a fast reaction between the La atoms in the bulk phase and the nickel particle can be expected. In the cases of the reductions of CeO_2, Pr_6O_{11} and Nd_2O_3, the reactions of Ce, Pr and Nd are prevented by the existence of a calcium-rich phase in the two-liquid region. The morphologies observed when the La-base and Ce-base $RmNi_5$ compounds were produced from their misch metal oxides by the R–D process [1–3] can be explained basically by this difference in the reaction mechanism between the reductions of La_2O_3 and CeO_2, Pr_6O_{11} or Nd_2O_3.

References

[1] Z. Li, K. Yasuda and K. Itagaki, *J. Min. Mater. Process. Inst. Jpn.*, *108* (1992) 33.
[2] K. Yasuda, Z. Li and K. Itagaki, *J. Min. Mater. Process. Inst. Jpn.*, *108* (1992) 103.
[3] Z. Li, K. Yasuda and K. Itagaki, *J. Alloys Compd.*, *192* (1993) 26.
[4] D.-Y. Kim, M. Ohtsuka and K. Itagaki, *J. Min. Mater. Process. Inst. Jpn.*, *108* (1992) 873.
[5] T.B. Massalski, *Binary Alloy Phase Diagrams*, Vol. 1, American Society for Metals, Metals Park, OH, 2nd edn., 1990, pp. 922, 902, 934.
[6] G. Qi, Z. Li, K. Itagaki and A. Yazawa, *Mater. Trans. Jpn. Inst. Met.*, *30* (1989) 583.
[7] M. Nortin and J. Hertz, *Acta Metall.*, *31* (1983) 903.